High precision optical characterization of semiconductor saturable absorber mirrors

D. J. H. C. Maas,[*] B. Rudin, A.-R. Bellancourt, D. Iwaniuk, S. V. Marchese, T. Südmeyer, and U. Keller

Department of Physics, Institute of Quantum Electronics, ETH Zurich, Wolfgang-Pauli-Str. 16, 8093 Zurich, Switzerland
[*]Corresponding author: maas@phys.ethz.ch

Abstract: Semiconductor saturable absorber mirrors (SESAMs) have become a key element of many ultrafast laser sources, enabling passively modelocked lasers with >100 GHz repetition rate or with >10 µJ pulse energy. Precise knowledge of the nonlinear optical reflectivity is required to optimize the SESAMs for self-starting passive modelocking at record high repetition rates or pulse energies. In this article, we discuss a new method for wide dynamic range nonlinear reflectivity measurements. We achieve a higher accuracy (<0.05%) with a simpler and more cost-efficient measurement scheme compared with previous measurement systems. The method can easily be implemented for arbitrary wavelength regions and fluence ranges.

©2008 Optical Society of America

OCIS codes: (140.4050) Mode-locked lasers; (230.4320) Nonlinear optical devices; (120.5700) Reflection.

References and links

1. U. Keller, K. J. Weingarten, F. X. Kärtner, D. Kopf, B. Braun, I. D. Jung, R. Fluck, C. Hönninger, N. Matuschek, and J. Aus der Au, "Semiconductor saturable absorber mirrors (SESAMs) for femtosecond to nanosecond pulse generation in solid-state lasers," IEEE J. Sel. Top. Quant. **2**, 435-453 (1996).
2. U. Keller, "Recent developments in compact ultrafast lasers," Nature **424**, 831-838 (2003).
3. U. Keller, "Ultrafast solid-state lasers," in *Landolt-Börnstein. Laser Physics and Applications. Subvolume B: Laser Systems. Part I*, G. Herziger, H. Weber, and R. Proprawe, eds. (Springer Verlag, Heidelberg, 2007), pp. 33-167.
4. L. Krainer, R. Paschotta, S. Lecomte, M. Moser, K. J. Weingarten, and U. Keller, "Compact Nd:YVO$_4$ lasers with pulse repetition rates up to 160 GHz," IEEE J. Quantum Electron. **38**, 1331-1338 (2002).
5. S. V. Marchese, C. R. E. Baer, A. G. Engqvist, S. Hashimoto, D. J. H. C. Maas, M. Golling, T. Südmeyer, and U. Keller, "Femtosecond thin disk laser oscillator with pulse energy beyond the 10-microjoule level," Opt. Express **16**, 6397-6407 (2008).
6. C. Hönninger, R. Paschotta, F. Morier-Genoud, M. Moser, and U. Keller, "Q-switching stability limits of continuous-wave passive mode locking," J. Opt. Soc. Am. B **16**, 46-56 (1999).
7. D. E. Spence, P. N. Kean, and W. Sibbett, "60-fsec pulse generation from a self-mode-locked Ti:sapphire laser," Opt. Lett. **16**, 42-44 (1991).
8. T. R. Schibli, E. R. Thoen, F. X. Kärtner, and E. P. Ippen, "Suppression of Q-switched mode locking and break-up into multiple pulses by inverse saturable absorption," Appl. Phys. B **70**, S41-S49 (2000).
9. R. Grange, M. Haiml, R. Paschotta, G. J. Spuhler, L. Krainer, M. Golling, O. Ostinelli, and U. Keller, "New regime of inverse saturable absorption for self-stabilizing passively mode-locked lasers," Appl. Phys. B **80**, 151-158 (2005).
10. S. C. Zeller, T. Südmeyer, K. J. Weingarten, and U. Keller, "Passively modelocked 77 GHz Er:Yb:glass laser," Electron. Lett. **43**, 32-33 (2007).
11. G. J. Spühler, K. J. Weingarten, R. Grange, L. Krainer, M. Haiml, V. Liverini, M. Golling, S. Schon, and U. Keller, "Semiconductor saturable absorber mirror structures with low saturation fluence," Appl. Phys. B **81**, 27-32 (2005).
12. S. V. Marchese, C. R. E. Baer, R. Peters, C. Kränkel, A. G. Engqvist, M. Golling, D. J. H. C. Maas, K. Petermann, T. Südmeyer, G. Huber, and U. Keller, "Efficient femtosecond high power Yb:Lu$_2$O$_3$ thin disk laser," Opt. Express **15**, 16966-16971 (2007).

13. D. Lorenser, D. J. H. C. Maas, H. J. Unold, A.-R. Bellancourt, B. Rudin, E. Gini, D. Ebling, and U. Keller, "50-GHz passively mode-locked surface-emitting semiconductor laser with 100 mW average output power," IEEE J. Quantum Electron. **42** (2006).
14. U. Keller and A. C. Tropper, "Passively modelocked surface-emitting semiconductor lasers," Phys. Rep. **429**, 67-120 (2006).
15. D. J. H. C. Maas, A.-R. Bellancourt, B. Rudin, M. Golling, H. J. Unold, T. Südmeyer, and U. Keller, "Vertical integration of ultrafast semiconductor lasers," Appl. Phys. B **88**, 493-497 (2007).
16. M. Haiml, R. Grange, and U. Keller, "Optical characterization of semiconductor saturable absorbers," Appl. Phys. B **79**, 331-339 (2004).

1. Introduction

During the last decade, semiconductor saturable absorber mirrors (SESAMs) [1] have become a key component for passively modelocked lasers [2, 3] and pushed the frontier for pulse repetition rates up to 160 GHz [4] and pulse energies to more than 10 µJ [5] for diode-pumped solid-state lasers. The SESAMs resolved the Q-switching instability problems for diode pumped solid state lasers because of their large absorption cross section [6]. Today, many different diode-pumped solid-state, fiber and semiconductor laser systems use a SESAM for modelocking because of the design flexibility: the SESAM can be designed for a broad wavelength and parameter range. In contrast to Kerr lens modelocking (KLM) [7] the SESAM provides reliable self starting and more flexibility in the laser cavity design because the laser does not need to be operated close to the stability limit.

A SESAM is a mirror structure with an integrated semiconductor saturable absorber, see Fig. 1(a). The absorber can be a bulk semiconductor, a quantum well or a layer consisting of quantum dots. These all have the same fundamental characteristic: they saturate at sufficiently high pulse energies which reduces the absorption and increases the reflectivity of the device. The SESAM has several important parameters, see Fig. 1(b): the modulation depth ΔR, i.e. the difference in reflectivity between a fully saturated and an unsaturated SESAM, the nonsaturable losses ΔR_{ns} and the saturation fluence F_{sat}, which is the pulse fluence (pulse energy per area) where the SESAM is saturated. All SESAMs have a maximum achievable reflectivity. If the fluence is larger than a certain value the reflectivity decreases for example through two-photon absorption (TPA) but also other effects. The parameter used to describe this induced absorption is F_2 [8, 9]. F_2 is the fluence where the reflectivity has dropped to 1/e due to induced absorption. It can be influenced by the SESAM design and depends on the pulse length of the measurement laser.

The optimum parameters for the SESAM strongly depend on the laser system. Q-switched modelocking (QML) instabilities are a major challenge for solid-state lasers operating at high repetition rates >10 GHz [6]. QML can be suppressed in many cases, if a SESAM with low modulation depth (<1%) and low saturation fluence is employed [10, 11]. On the other hand for high pulse energy lasers (i.e. >1 µJ), SESAMs with a large saturation fluence are more favorable because it facilitates the cavity design [12]. Induced absorption can reduce modelocking instabilities due to QML [9]. However, the induced absorption can also limit the maximum achievable pulse energy, if the roll-over occurs at lower pulse fluence [5].

For vertical external cavity surface emitting lasers (VECSELs) we also need saturable absorbers with a small saturation fluence [13, 14]. In contrast to diode-pumped solid-state lasers where we do not have any dynamic pulse-to-pulse gain saturation the absorber additionally needs to saturate faster than the gain for stable modelocking. Quantum dot SESAMs have become relevant to resolve this issue for wafer scale integration of the saturable absorber with the gain in a passively modelocked surface emitting semiconductor laser [15].
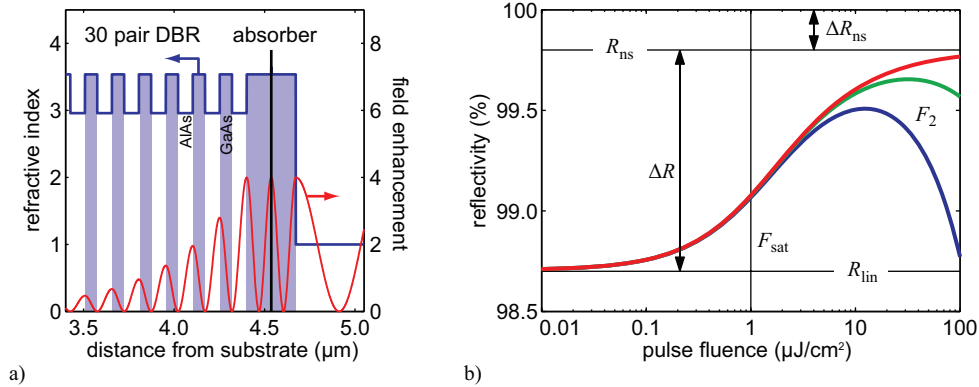
Fig. 1. (a) A typical SESAM design. The structure contains a 30 pair distributed Bragg reflector with a saturable absorber grown on top. (b) Reflectivity as function of the incident pulse fluence. Initially, the reflectivity increases with pulse fluence. Inverse saturable absorption can lead to a roll-over and decreases the reflectivity for high fluences. The blue curve has a small induced absorption parameter F_2, the green curve has a large F_2 and for the red curve $F_2 = \infty$.

For diode-pumped solid-state lasers and surface emitting semiconductor lasers a small modulation depth of typically 0.5% is sufficient for self-starting passive modelocking, and a low nonsaturable losses of <0.1% is required for low output coupling and to reduce excessive thermal heating which becomes even more severe for more than 100 W of intracavity average power levels. Therefore, a precise knowledge of the SESAM absorber parameters is crucial for state-of-the-art modelocked laser sources. However, such measurements are challenging because such a small change of reflectivity (e.g. 0.5%) has to be measured with sufficient accuracy over the full dynamic range of about 4 orders of magnitude in pulse fluence.

Previously, Haiml et al. demonstrated a measurement system for the optical characterization of semiconductor saturable absorbers [16]. The core of the setup is a beam splitter (an uncoated small-angle wedged glass plate) in front of the SESAM (see Fig. 2). The reflection on the front side (A) is proportional to P_{in} and the reflection on the back side (B) is proportional to $R\,P_{in}$. The reflectivity of the SESAM is $R = B / A$ and can be computed as function of the incident pulse fluence, which is changed by a variable attenuator through a combination of a half-wave plate, a polarizer and an acousto-optic modulator (AOM). The detectors must be able to measure voltages over at least four orders of magnitude with an accuracy of better than 0.1%. A lock-in detection with two separate lock-in amplifiers has to be used to reduce the influence of stray light and noise. The AOM is used for modulation of the incident beam required for the lock-in scheme. However, it is very challenging to achieve sufficient accuracy, because the required performance is close to the linearity limit of the lock-in amplifiers.
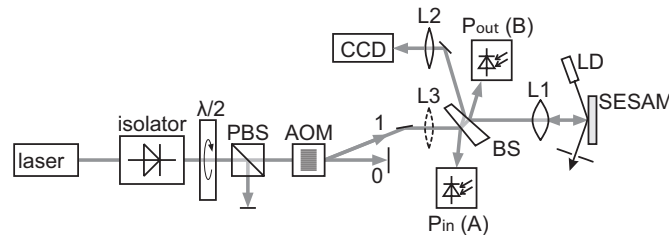

Fig. 2. Previous setup according to Ref. [16]: the attenuation is a combination of an half wave-plate and an AOM. The core of the setup is the beamsplitter (BS) that separates the incident (P_{in}) and reflected beam (P_{out}).

Here we present a new approach: instead of detecting A and B simultaneously by two different detectors, these signals are separated in time and measured with the same detector system. This way, we can improve the accuracy and linearity, while at the same time reducing the requirements on the measurement system. We achieve an accuracy of less than 0.05% for an incident pulse fluence varied over more than four orders of magnitude.

In section 2, we introduce the new measurement method and discuss design considerations for the separate parts. In Section 3, the computation of the measurement data is described, and in section 4 we describe the alignment and calibration. The results of measurements with two different laser systems are shown in section 5. Finally the conclusions and an outlook are given in section 6.

2. Measurement concept

The nonlinear reflectivity measurement system consists of several parts, a pulsed laser source, a variable attenuator, an isolator and finally the measurement section (Fig. 3).
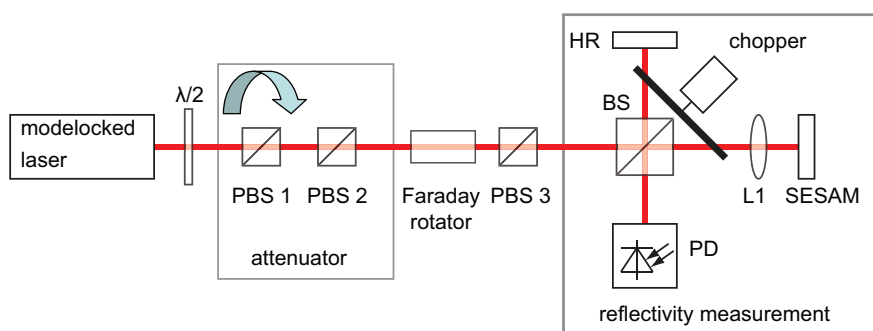

Fig. 3. The experimental setup: the output of the pulsed laser source propagates through a variable attenuator to set the pulse energy, then through the isolator to eliminate back reflections and finally enters the measurement part. The reflectivity of the SESAM is obtained by measuring the response from both arms and computing the ratio.

The pulsed laser source typically is a modelocked laser with sufficient energy to saturate the SESAM under test. Ideally, we want to characterize the SESAM under identical conditions as inside a laser cavity that is passively modelocked by the same SESAM. The pulsed laser source should therefore operate at the same center wavelength and pulse duration. The pulse fluence incident on the SESAM should be at least 10 times F_{sat} for a precise parameter extraction [16], but depending on the induced absorption (e.g. a large F_2) fluences of up to 50 times F_{sat} can be required for a precise characterization. In a modelocked laser, the intracavity fluence on the SESAM is typically 3-10 times F_{sat}. So we need to achieve approximately the same or higher fluence than inside the cavity. This is usually obtained either by strong focusing onto the SESAM or employing a lower repetition rate of the evaluation laser. At high repetition rates, some SESAMs do not fully recover between the subsequent laser pulses, and an evaluation at the precise repetition rate may even be needed.

A wide-dynamic range attenuator can be realized in many ways, e.g. by graded neutral density filters, acousto-optical modulators (AOMs), or polarization splitters in combination with polarization rotation optics. Neutral density filter wheels, however, may cause thermal lensing at high average power levels. AOMs can introduce amplitude noise at stronger attenuation levels and are typically limited to two orders of magnitude of attenuation. In our setup, we choose to use the polarization method, which relies on two optical elements: one element rotates the linear polarization state, whereas the second element selects the desired polarization. Polarization rotation can be achieved using for example a half-wave plate or a polarizing beam splitter (PBS). Because half-wave plates typically have a limited bandwidth,

we prefer to use PBSs which have a bandwidth >100 nm. The dynamic range is determined by the extinction ratio of the first PBS.

The angle of incidence onto the SESAM is perpendicular, and hence some light is reflected back into the laser source. An isolator prevents such back-reflections from entering the laser source, which would lead to modelocking instabilities. The isolator consists of two polarizing beam splitters PBS2 and PBS3 and a faraday rotator. To obtain good isolation we used Glan Laser PBSs, which have a 250 nm – 2.3 µm wavelength range and a extinction ratio of 1:100,000.

The measurement part consists of a non-polarizing beam splitter cube (BS), a lens, a chopper wheel and a photo detector (PD). Instead of detecting A and B simultaneously by two different detectors (like Haiml et al [16]), the signals are separated in time and measured with the same detector system. The separation in time is achieved by a chopper wheel which simultaneously chops both arms and is put close to the 50:50 beamsplitter. The signal is amplified and measured with an analog-to-digital (AD) converter and recorded with a computer. The chopper frequency is typically in the range of 100s of Hertz, and a low-cost 14 bit AD-converter is sufficient to measure photovoltages with 0.01% accuracy (when the photo-current amplifier is set to obtain a full-scale for the reference signal, 14 bits results in 0.006% resolution, averaging over more points can even increase this value).

In our measurement system, we lifted the chopper wheel such that the axis of the chopper wheel is a few centimeters above the beam heights, see Fig. 4(a). During one chopper wheel cycle, four different states occur: 1. only reference beam measured, 2. both beams measured, 3. only sample beam measured, and 4. both beams are blocked. The signal in phase 4 corresponds to a background signal from photodiode dark current and environmental background light, which is then discriminated from the measurement signal in phase 1 and 3. In reference [16], a lock-in detection was required to reject the background signal.

The lens L1 focuses the incident beam onto the SESAM, typical beam radii are between 5 µm and 20 µm. We employ a photo detector with a large detection area (typically 7x7 mm) to measure a collimated beam with large beam radius.

3. Data evaluation

The PD signal is amplified by a computer-controlled variable pre-amplifier to use the full range of the AD converter. The absolute gain and the offset have no influence on the measurement accuracy, it is only necessary to provide a linear response. Since the reflectivity R is encoded in only one optical/electrical signal the constraints on the amplifier have become negligible. This is in contrast to the method of Haiml et al., in which the same gain and no offset has to be achieved by both amplifiers [16].

The computer algorithm first detects the rising edges (red dots in Fig. 4(b)) and then takes the mean value of the data points on the flat levels (red lines in Fig. 4(b)). As both beams are blocked in phase 4, we can precisely measure the offset of the photodiode. Level A and B (Fig. 4(b)) are obtained by subtracting the signal level in state 1, and the nonlinear reflectivity is obtained as $R = B / A$. This is done for 500 periods in succession (takes approximately 5 seconds per fluence) and averaged to minimize detector noise and laser noise. This averaged reflectivity has a standard deviation of 0.01%. The incident fluence can be computed from the level A and the pre-amplifier gain setting. An accuracy of 5% for the fluence measurement is typically good enough, as this will afterwards result in an inaccuracy of 5% for the fitted saturation fluence F_{sat}.
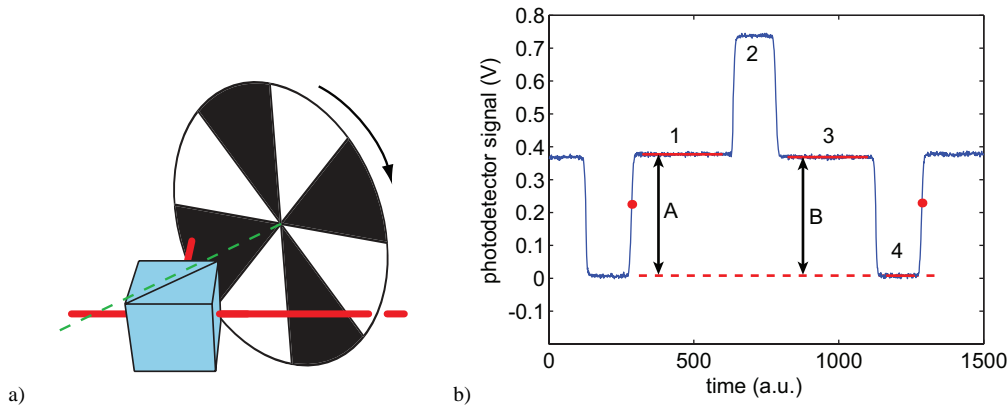
Fig. 4. (a) The chopper wheel is lifted a few centimeters to block both beams at certain angles, which makes it possible to measure the photodiode offset and (b) the corresponding trace on the photodiode.

4. Alignment and calibration

In this section, we first give a guideline for the optical design and initial alignment, then describe the steps to prepare the setup for measurements: calibration of the reflectivity, alignment of the SESAM to make sure it is in the focus of the laser beam and the exchange of the SESAM.

The beam splitter as well as all the other optical components are slightly tilted to eliminate reflections from the interfaces hitting the photodiode. We observed up to 2% measurement error when parasitic reflections or scattered light reached the detector, preventing such reflections from hitting the detector is therefore particularly important.

To achieve an identical optical-to-electrical response of the detector from the sample beam and the reference beam, the setup is designed in such a way that both beams have an identical spot size on the photodiode. The beam that enters the reflectivity measurement part is collimated and has a waist (1 mm radius) on the reference mirror. The sample beam is focused onto the sample using lens L1. Both returning beams have the same q parameter (beam width and divergence). The overlap of both backward traveling beams can be verified by using a camera at the detector position.

An obvious sanity check is the measurement of a HR instead of the SESAM in the sample arm, which should result in a flat response over the full dynamic range. Because the sample arm includes an additional lens, the response from this arm is typically a few percent lower than the response from the reference arm. We introduce a calibration factor such that the reflectivity $R = C \cdot B / A$ is constant. In case of systematic errors C can be a function of the fluence F.

For a measurement, the SESAM has to be positioned at the waist at zero degree incidence. First the SESAM is aligned perpendicular to the beam without the lens L1 by using an aperture. Then the lens is inserted and the beam is aligned again to the aperture. The final alignment concerns the fine tuning of the SESAM position, which needs to be exactly in the focus of the laser beam. Here we use the same procedure as described by Haiml et al., where the SESAM is moved along the propagation direction and the beam waist is where the nonlinearity is the largest and thus the measured saturation fluence is the smallest [16].

One has to be careful when replacing the sample, because slight misalignments can result in measurement errors. We therefore use two alignment beams from a laser pointer to memorize the sample position and tilting angle (see Fig. 5): the first beam is reflected by the sample and is directly aligned to an aperture; the second beam propagates through two lenses (focal length 5 cm) with the sample in-between. A linear translation of the sample causes a

deviation in the angle of the collimated output beam that is aligned to a second aperture. The first beam is sensitive to angular errors and has a reproducibility better than 30 mrad. The second beam is mainly sensitive to position errors and has a reproducibility of 10 µm which is well below the Rayleigh length (140 µm). We obtain a 0.02% reproducibility of the reflectivity measurement.
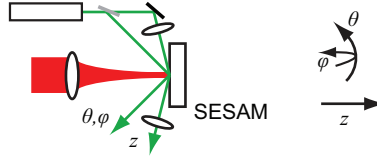

Fig. 5. Two alignment beams are used to guarantee the reproducibility of the sample position.

5. Results

5.1 Evaluation and Fit Function

We use a model function to fit the measurement data. The function is derived using a rate equation describing a two-level system (i.e. valence band and conduction band) [16]. The model takes into account the absorption of photons, but neglects the recombination, which is a good model for a slow saturable absorber where the recovery time is longer than the pulse duration. But also SESAMs with a fast recovery can usually be described with the deducted nonlinear reflectivity curve. To take into account induced absorption at higher fluences the model function is multiplied with a correction factor $\exp(-F/F_2)$, where F_2 is the induced absorption coefficient. This results in

$$R(F) = R_{ns} \frac{\ln\left[1 + R_{lin}/R_{ns}\left(e^{F/F_{sat}} - 1\right)\right]}{F/F_{sat}} e^{-\frac{F}{F_2}} , \qquad (1)$$

where $F(x, y)$ is still a function of the spatial coordinates. To obtain the reflectivity from a pulse with a Gaussian beam profile and the fluence defined as $F_p = E_p / (\pi\, w^2)$, we have to integrate (1) over the entire beam profile and obtain

$$R^{Gauss}(F_p) = \frac{1}{2F_p} \int_0^{2F_p} R(F)\, dF . \qquad (2)$$

R^{Gauss} can only be computed numerically. To compare the model function with measurement data we define the distance σ as the squared 2-norm of the difference between the measured reflectivity and the reflectivity of the fit curve. The best fit has the smallest σ.

5.2 VECSEL source

The first setup was built for the characterization of low saturation fluence quantum dot SESAMs which are used to passively modelock VECSELs [13] and which have been integrated into the modelocked integrated external-cavity surface emitting laser (MIXSEL) [15]. The measurement was performed using a VECSEL with 1 W of average output power at 960 nm. The VECSEL is modelocked with a SESAM at 1.5 GHz and generates 6-ps-long pulses. We focused the beam with a 20 mm lens to a small spot with a 5.8 µm radius. The fluence range is only three orders of magnitude, from 0.2 – 200 µJ/cm^2 since we were limited by the maximum pulse energy available from this gigahertz repetition rate laser. A typical measurement, which takes approximately 2 minutes, is shown in Fig. 6(b). A dielectric HR was used for calibration. The reference measurement on this mirror shows peak-to-peak variation (flatness) of only 0.049%, see Fig. 6(a). The data is fitted with a logarithmic function (straight line on a semi-logarithmic axis) which is used to correct following

measurements. The SESAM is a quantum dot SESAM with a resonant design [11]. At low fluences we have a linear response of the dots, whereas at higher fluence we increase the carrier population due to the rather long recombination time and therefore increase the reflectivity of the SESAM due to the decreased absorption and increased stimulated emission. Due to the rather long 6 ps-pulses there is no induced absorption (for the fit we use $F_2 = \infty$) and three orders of magnitude are sufficient for a good fit. From the fit we determine the modulation depth to be $\Delta R = 2.17 \pm 0.02\%$ (the tolerance corresponds to standard deviation of the fit parameter), the nonsaturable losses $\Delta R_{ns} = 1.23 \pm 0.02\%$ and the saturation fluence $8.48 \pm 0.36\ \mu J/cm^2$.
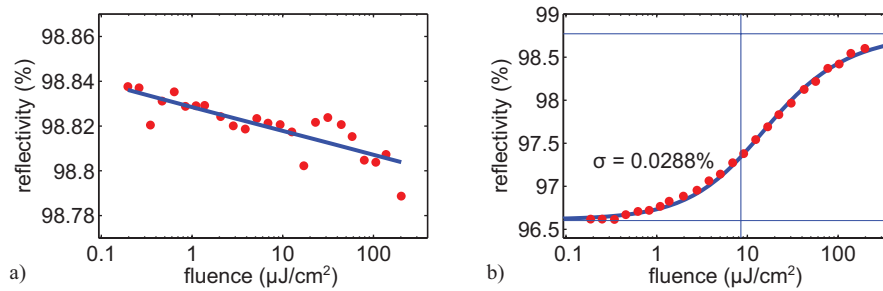

Fig. 6. (a) Measurement of a HR without calibration (i.e. $C = 1$), the flatness of the mirror is below <0.05% and (b) a typical SESAM measurement.

5.3 Thin Disk laser source

The second setup was built for the evaluation of high saturation fluence SESAMs operating at 1030 nm, which enabled the realization of passively modelocked thin disk lasers exceeding 10 µJ pulse energy [5]. The SESAM has InGaAs quantum wells which absorb the laser light. At a sufficient fluence the carriers start filling the bands and the wells become transparent. The laser source is a modelocked Yb:Lu$_2$O$_3$ thin disk laser running at a lower repetition rate of 65 MHz [12]. The pulses are 570-fs long, which will cause induced saturable absorption at higher fluences. We used a lens with a focal length of 25 mm to obtain a 10.3 µm beam waist (radius) on the sample, which allowed measurements up to 6800 µJ/cm^2. The HR flatness was improved by choosing $C(F)$ as a second order polynomial of $\log(F)$. The HR measured with this correction factor has a flatness of 0.055%, see in Fig. 7. From the fit we obtained $F_{sat} = 54.7 \pm 1.4\ \mu J/cm^2$, $\Delta R = 0.722 \pm 0.005\%$, $F_2 = 3.18 \pm 0.13\ J/cm^2$ and very small nonsaturable losses $\Delta R_{ns} = -0.003 \pm 0.005\%$. The systematic error in the measurement of the nonsaturable losses ΔR_{ns} depends on the accuracy of the HR reference measurement (see section 4), therefore we can only conclude that $\Delta R_{ns} < 0.1\%$. The green curve in Fig. 7 shows the same fit function with $F_2 = \infty$, i.e. the expected reflectivity for ps-pulses.
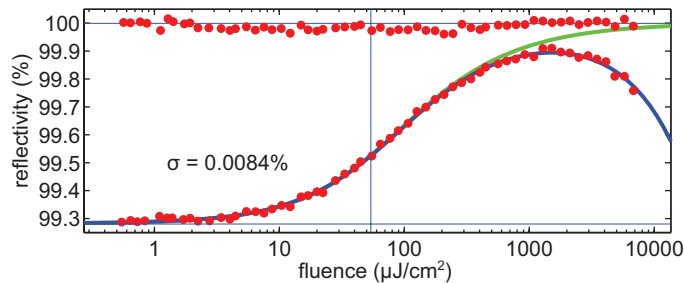

Fig. 7. Measurement of a HR with calibration, the reflectivity is close to 100% with a flatness of 0.055% and a SESAM measurement with small modulation depth, measured over four orders of magnitude. The green curve shows the fit function without induced absorption.

6. Conclusion and outlook

We present a new tool for the characterization of the nonlinear reflectivity of SESAMs with a higher accuracy and lower constraints on electronic equipment. Instead of two photodiodes and two high-end lock-in amplifiers only one photodiode, a simple amplifier and an AD converter are needed to obtain measurements with better accuracy. Despite the simple and cost-efficient approach, an accuracy of <0.05% is achieved over a dynamic range of more than a factor of 10^4. Care has to be taken in the alignment, since parasitic reflections and scattered light can cause relatively large errors. To exchange the sample we set up two alignment laser beams to make the measurement very reproducible. So far the setup has been tested with two laser systems: a VECSEL at a high repetition rate and a thin disk laser generating pulses with high energy.

Such highly accurate measurements are required for state of the art modelocking results. In future we want to further optimize SESAMs and study the influence of spot-size, repetition rate and pulse length on the macroscopic SESAM parameters.